

pubs.acs.org/acschemicalbiology Articles

# Allele-Specific Chemical Rescue of Histone Demethylases Using Abiotic Cofactors

Published as part of the ACS Chemical Biology Young Investigators virtual special issue

Valerie Scott, Debasis Dey, Jordan Kuwik, Kathryn Hinkelman, Megan Waldman, and Kabirul Islam\*



Cite This: ACS Chem. Biol. 2022, 17, 3321–3330



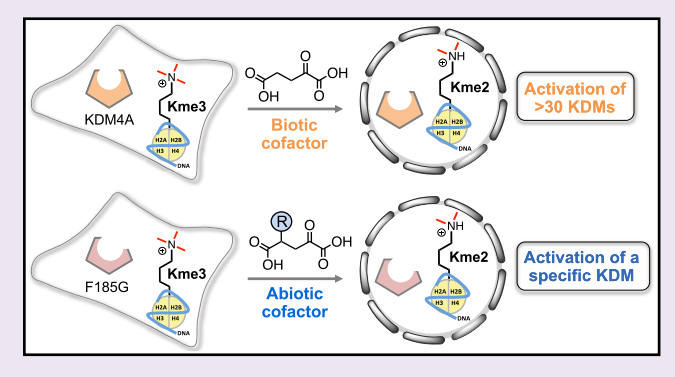
**ACCESS** I

III Metrics & More

Article Recommendations

Supporting Information

**ABSTRACT:** Closely related protein families evolved from common ancestral genes present a significant hurdle in developing member- and isoform-specific chemical probes, owing to their similarity in fold and function. In this piece of work, we explore an allele-specific chemical rescue strategy to activate a "dead" variant of a wildtype protein using synthetic cofactors and demonstrate its successful application to the members of the alpha-ketoglutarate ( $\alpha$ KG)-dependent histone demethylase 4 (KDM4) family. We show that a mutation at a specific residue in the catalytic site renders the variant inactive toward the natural cosubstrate. In contrast,  $\alpha$ KG derivatives bearing appropriate stereoelectronic features endowed the mutant with native-like demethylase activity while remaining refractory to a set of wild type dioxygenases. The



orthogonal enzyme-cofactor pairs demonstrated site- and degree-specific lysine demethylation on a full-length chromosomal histone in the cellular milieu. Our work offers a strategy to modulate a specific histone demethylase by identifying and engineering a conserved phenylalanine residue, which acts as a gatekeeper in the KDM4 subfamily, to sensitize the enzyme toward a novel set of  $\alpha$ KG derivatives. The orthogonal pairs developed herein will serve as probes to study the role of degree-specific lysine demethylation in mammalian gene expression. Furthermore, this approach to overcome active site degeneracy is expected to have general application among all human  $\alpha$ KG-dependent dioxygenases.

#### INTRODUCTION

Lysine demethylases (KDMs) are alpha-ketoglutarate ( $\alpha$ KG)dependent dioxygenases that use Fe2+ to catalyze the removal of methyl groups in histones to regulate gene expression (Figure 1A).<sup>1-3</sup> More than 30 KDMs partake in diverse cellular processes ranging from chromatin organization to nuclear reprogramming during cellular differentiation, all occurring at a wide range of time scales (Figures S1 and S2).<sup>1-3</sup> Overexpression and somatic mutation of KDMs are hallmarks of various human cancers.4 How a specific KDM member contributes to distinct gene expression patterns in normal and pathological conditions is largely unexplored, likely because interrogating KDM-specific functions in the spatiotemporally fluctuating environment of cells is challenging. We reasoned that catalytic activation of an otherwise dead KDM mutant would constitute a powerful approach for the gain-offunction study of degree-specific lysine demethylation (Figure 1B). Such allele-specific activation is unlikely to be attained by pharmacological or genetic perturbations alone since these approaches typically lead to a catalytic loss of the demethylases and fail to provide insights into the causal role of lysine demethylation in biological processes.

Activation of enzyme function with small molecules is an underutilized approach in chemical genetics, mainly because of the significant thermodynamic burden in restoring the catalytic steps. The earlier strategy toward allele-specific enzyme activation involves the introduction of a *de novo* pocket in the catalytic domain of an enzyme to render it nonfunctional, followed by the chemical rescue of activity with a small molecule through stereoelectronic complementarity. Such an approach, however, may pose certain limitations as high concentrations of biotic activators (e.g., imidazole, indole) are used to induce the desired phenotype, which can potentially interfere with the inherent metabolic processes of the cell. We envisioned developing an analogue-sensitive chemical rescue strategy using abiotic cofactors (e.g.,  $\alpha$ KG derivatives) that are orthogonal to the wild type KDMs to specifically activate an

Received: May 6, 2021
Accepted: August 26, 2021
Published: September 8, 2021





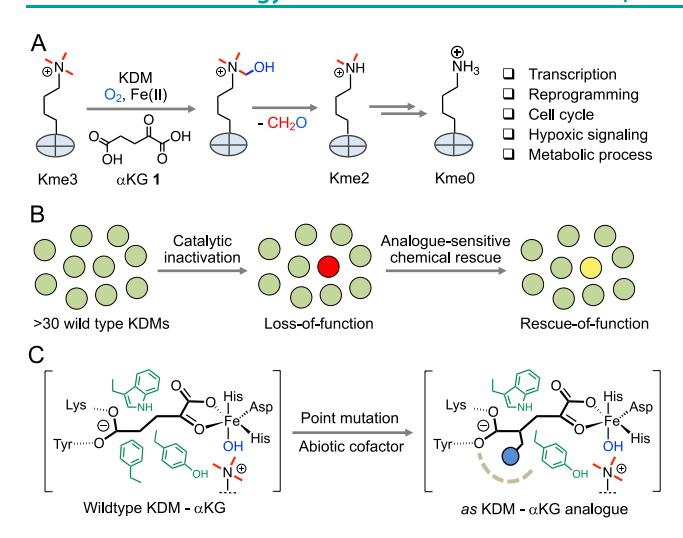


**Figure 1.** Analogue-sensitive (as) chemical rescue of KDMs. (A) Biochemical steps involving oxidative histone demethylation by KDMs and  $\alpha$ KG. (B) Schematic representation of a two-step strategy for analogue-sensitive (as) activation of KDMs: First catalytic inactivation of a specific member followed by chemical rescue with a cofactor analogue as shown in C. (C) Sketch showing binding of  $\alpha$ KG in the active site of native KDM (left) and that of an  $\alpha$ KG analogue (an abiotic cofactor) into an expanded active site of the as variant (right).

otherwise silent KDM variant (Figure 1C). <sup>13</sup> We reasoned that a space-creating mutation at a bulky hydrophobic residue in the active site would result in an inactive allele, which could then be resurrected by cofactor mimetics with appropriate steric appendages. Such steric engineering between an enzyme and its cofactor would be thermodynamically less intrusive for maintaining a productive catalytic cycle, as the majority of electrostatic interactions would remain intact.

We recently showed that the steric component of the KDM4A and  $\alpha$ KG interface can be remodeled in a

complementary manner to access an orthogonal demethylation apparatus. <sup>14</sup> Herein, we expand our earlier observation to all five catalytically active members of KDM4 subfamily, identify a conserved gatekeeper residue in the active site, and explore a new set of  $\alpha$ KG analogues for member-specific functional analysis. First, we develop an approach toward regioselective synthesis of  $\alpha$ KG derivatives bearing diverse steric appendages at C4. Subsequent biochemical experiments lead to several enzyme-cofactors pairs for the KDM4 family with improved orthogonality and catalytic proficiency. Finally, we demonstrate activation of a specific KDM4 member in the complex cellular milieu using the abiotic cofactors to modulate lysine demethylation in chromosomal histones in a site- and degree-specific manner.

# ■ RESULTS AND DISCUSSION

Synthesis of  $\alpha$ KG Analogues Carrying Hydrophobic **Appendages.** KDM4A harbors the *ImjC* catalytic domain that utilizes  $\alpha KG$  and  $Fe^{2+}$  to demethylate lysine residues in histones. 15 Within the binding pocket, F185 resides in close proximity ( $\sim$ 3 Å) to  $\alpha$ KG, specifically to the C4 methylene unit of the cofactor (Figure 2A). 16 We previously revealed that F185G mutation led to a complete loss of activity toward the canonical  $\alpha$ KG, and the demethylase activity could be rescued with cofactor analogues primarily via steric complementarity.<sup>14</sup> To expand the cofactor repertoire and enhance their orthogonality across human  $\alpha$ KG-dependent enzymes, we designed a set of  $\alpha$ KG analogues 2–9 carrying distinct alkyl, alkenyl, alkynyl, and aryl groups with varied sizes at C4 (Figure 2B). We developed a short synthetic approach to access these molecules, which commenced from unprotected  $\alpha$ KG (Figure 2C, Schemes S1-S6). Acid-catalyzed protection of the carboxylic and 2-oxo groups present in 1 with orthoformate led to the diester-ketal 10. Subsequently, regioselective S<sub>N</sub>2 alkylation at C4 with varied electrophiles carrying a  $\beta_1 \gamma_2$ unsaturation provided a fully protected, racemic mixture of the

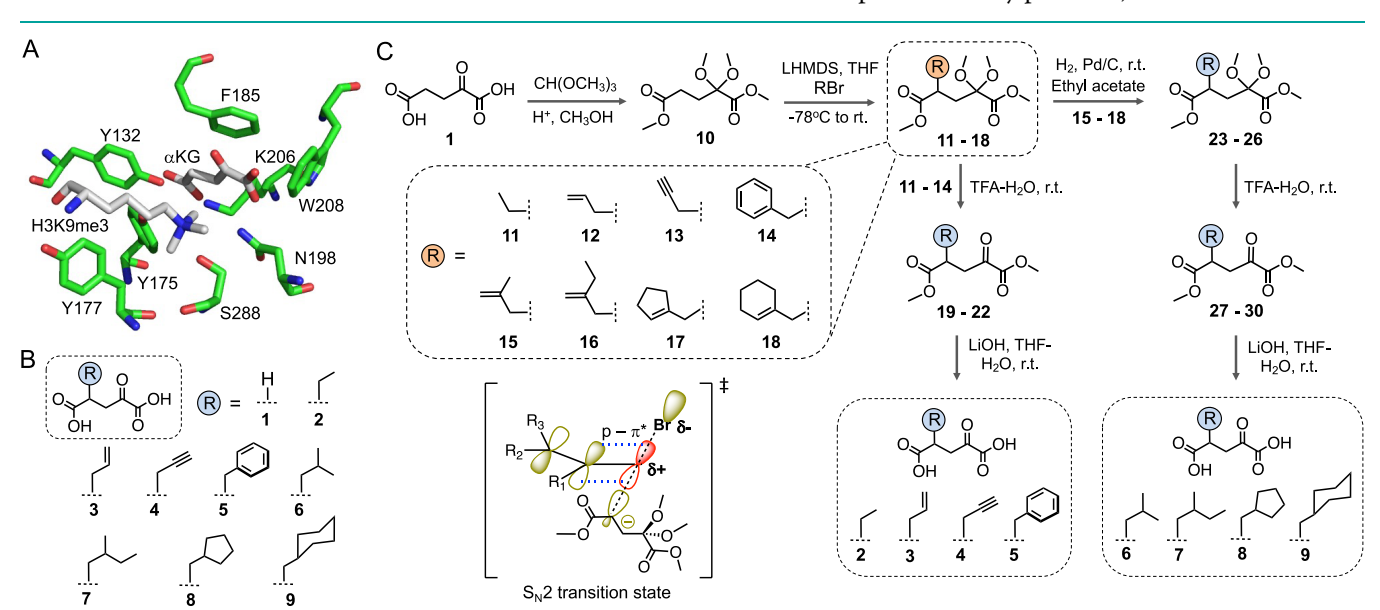


Figure 2. Design and synthesis of  $\alpha$ KG analogues. (A) Crystal structure of  $\alpha$ KG- and H3K9me3-bound catalytic domain of KDM4A (PBD: 2Q8C). (B) Structures of  $\alpha$ KG analogues 2–9 carrying a bulky hydrophobic moiety at C4. (C) Synthetic scheme toward  $\alpha$ KG analogues 2–9. Yields of the individual chemical transformations are provided in the Supporting Information. In the proposed linear transition state of S<sub>N</sub>2 alkylation, sp<sup>3</sup>-hybridized methylene carbon bearing a leaving group (Br) is rehybridized to sp<sup>2</sup> and the incipient p orbital is stabilized through delocalization with an adjacent antibonding  $\pi$  orbital (p- $\pi$ \* delocalization) of the  $\beta$ - $\gamma$  unsaturated electrophiles.

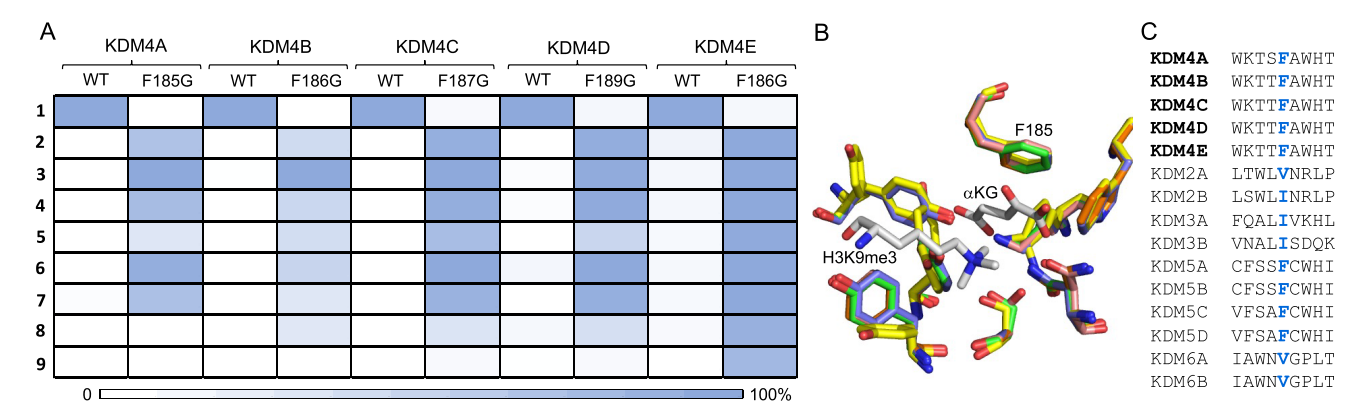


Figure 3. Development of analogue-sensitive (as) KDM4 demethylases. (A) Heat-map representation of % activity of KDM4A–E and corresponding mutants toward  $\alpha$ KG 1 and analogues 2–9. (B) Superimposed crystal structures of KDM4A–E showing a conserved binding pattern (PDB codes for KDM4A, 2Q8C; KDM4B, 4LXL; KDM4C, 4XDO; KDM4D, 4HON; KDM4E, 2W2I). (C) Structure-based sequence alignment of selected members of human KDMs showing conserved hydrophobic residues corresponding to F185.

 $\alpha$ KG analogues 11–18. The rationale behind the employment of unsaturated electrophiles was to facilitate the alkylation step by lowering the transition state barrier through p- $\pi^*$  delocalization known as allylic stabilization. Acid-catalyzed deketalization of 11–14 to 19–22 followed by ester hydrolysis led to the final analogues 2–5 (Figure 2C). Catalytic hydrogenation of the side chains on 15–18 led to the saturated intermediates 23–26 followed by both acid- and base-catalyzed deprotection furnished the  $\alpha$ KG analogues 6–9, which were purified using high performance liquid chromatography (Figure 2C).

Assessing  $\alpha$ KG Analogues As Alternative Demethylase Cofactors. We next sought to examine if the  $\alpha$ KG derivatives could rescue demethylase activity of the F185G mutant, an inactive variant of KDM4A toward the natural cofactor. The analogues were tested for their ability to activate the mutant to demethylate an H3K9me3 substrate peptide, and each product was analyzed by MALDI-TOF MS. To evaluate the relative product distribution, we first examined if the peptides carrying degree-specific methyllysine (Kme0, Kme1, Kme2, and Kme3) produced comparable ionization potentials. For this, we synthesized three additional peptides (H3K9me0, H3K9me1, and H3K9me2; Figures S3-S6). H3K9me3 was mixed with each synthesized peptide separately in different ratios and subjected to MALDI-MS. Peak intensities of individual peptides reflected their known ratios in the mixture, indicating equivalent degrees of ionization in MALDI (Figures S3-S6). Such a result suggests that a MALDI-based detection method can be employed for relative quantification of demethylase activity.

When examined using our optimized *in vitro* MALDI-based assay, most of the synthesized cofactor analogues activated the mutant, albeit to varied degrees; in contrast, they failed to induce demethylase activity in the wild type KDM4A, thus providing several orthogonal enzyme-cofactor pairs (Figures 3A, S7, S8). Ethyl (2), allyl (3), propargyl (4), isobutyl (6), and 2-methylbutyl (7) analogues proved to be the most promising cofactors, as their addition led to complete consumption of the substrate peptide. The benzyl  $\alpha$ KG (5) with a planar phenyl moiety activated the mutant enzyme moderately.  $\alpha$ KG analogues such as cyclopentylmethyl 8 and cyclohexylmethyl 9 were inactive, likely due to their cyclic and rigid side chains that led to steric congestion at the active site. It is remarkable that the engineered pair displayed degree-

specific demethylation (H3K9me3 to H3K9me2), consistent with monodemethylase activity of the wild type system. Furthermore, the demethylation was site selective as the mutant failed to demethylate H3K4me3 and H3K27me3 (Figures S9–S11), corroborating well with the activity of their wildtype congener. Collectively, by screening a set of novel  $\alpha$ KG analogues, we expanded the repertoire of active cofactors for the F185G mutant. The unique geometric and steric features present in the analogues are expected to improve the orthogonality of the abiotic cofactors across human  $\alpha$ KG-dependent dioxygenases.

Engineering F185 Equivalent Residue in KDM4B-E. The KDM4 subfamily consists of five catalytically active members (4A-E) and one pseudogene (4F; Figure S2). KDM4A-E, with multidomain structures, performs distinct functions in DNA damage response and nuclear reprogramming pathways which are attributed to their differential cellular localization, substrate selection, and catalytic properties (Figure S2).<sup>17-19</sup> Sequence analysis revealed that F185 of KDM4A is highly conserved among the human KDM members, and structurally occupies a position similar to F187 in KDM4C and F189 in KDM4D (Figure 3B, C). 20-23 This amino acid likely acts as a gatekeeper that precludes binding of a bulky  $\alpha$ KG analogue to wild type demethylases. To develop analogue-sensitive variants for all of the members, we generated the corresponding F185G mutation in KDM4B-E, expressed the mutant proteins, and examined their demethylase activity with the same set of synthesized  $\alpha KG$ analogues using MALDI-TOF MS (Figures 3A, S12-S19). In the end-point assay, wild type KDM4B-E proteins showed robust activity with canonical  $\alpha$ KG and remained vastly inactive toward the bulky αKG congeners (<5% H3K9me3 demethylation), confirming orthogonality of the analogues across the KDM4 family. On the other hand, the cofactor derivatives successfully activated the mutants to demethylate the H3K9me3 peptide. Mutants displayed varied degrees of analogue sensitivity while remaining refractory toward aKG itself. For example, allyl  $\alpha KG$  (3) effectively activated all of the variants in contrast to ethyl  $\alpha KG$  (2) and isobutyl  $\alpha KG$  (6), which proved to be the superior analogues for the KDM4C mutant. Remarkably, cyclopentylmethyl  $\alpha KG$  (8) and cyclohexylmethyl  $\alpha$ KG (9), which were inactive toward KDM4A-F185G, appeared to be potent cofactors for KDM4E-F186G (Figures 3A, S12-S19). Overall, the variants demonstrated

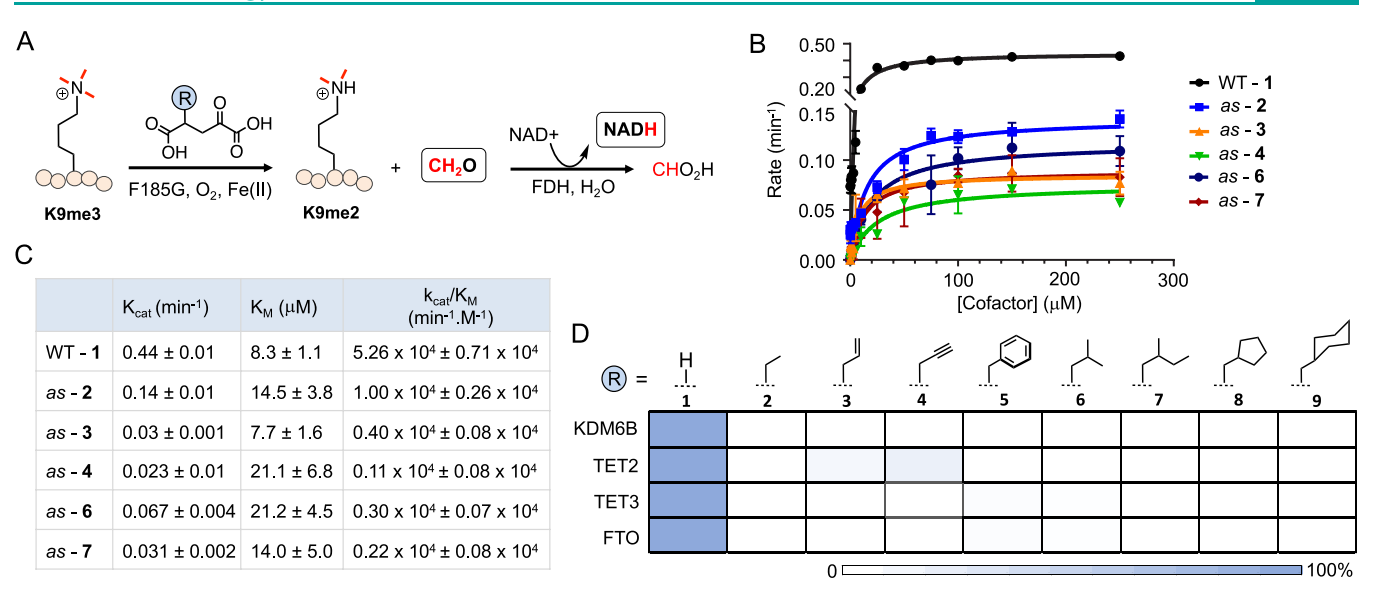


Figure 4. Kinetic parameters of analogue-sensitive (as) KDM4A and  $\alpha$ KG analogues. (A) Biochemical steps showing a coupled fluorescence assay involving oxidative histone demethylation by as pairs followed by oxidation of formaldehyde by formaldehyde dehydrogenase (FDH) to generate NADH. (B) Michaelis—Menten plots for wildtype and selected as pairs. (C) Kinetic parameters ( $k_{cat}$  and  $K_{M}$ ) obtained from B. (D) Selectivity of the  $\alpha$ KG analogues toward representative histone, DNA, and RNA demethylases.

differential analogue sensitivity, reflecting the structural and biochemical nuances of the KDM4 members. Taken together, we developed a functional variant for each member of the KDM4 family by screening an extended set of  $\alpha$ KG analogues against the variants carrying a single mutation at the gatekeeper residue. Given that the bulky hydrophobic residue is highly conserved among human KDMs, we surmise that the allelespecific chemical rescue approach is applicable to members of the entire KDM family.

Kinetic Assessment of Mutant-Cofactor Pairs. The lysine methylation-demethylation cycle is a dynamic process that controls transcriptional activity within cells in response to internal and external stimuli. Although the steady-state half-life of methylated histones is on the order of days, demethylation occurs rapidly at certain loci within minutes upon appropriate activation. 24-27 To examine the catalytic efficiency of the engineered demethylase pairs, we employed a coupled fluorescence assay that measures the amount of formaldehyde resulting from KDM-mediated C-H hydroxylation of the lysine methyl groups (Figures 4A, S20). In this assay, formaldehyde dehydrogenase (FDH) converts formaldehyde to formic acid by utilizing NAD+ and generating NADH in the process.<sup>28</sup> Accumulation of NADH was monitored using its intrinsic fluorescence, excitation at 340 nm, and emission at 490 nm, to quantify formaldehyde generation. We focused on the F185G mutant of KDM4A and selected cofactors that showed significant activity during the initial screening assay. The kinetic measurements were conducted at a saturating concentration (300  $\mu$ M) of the peptide substrate, which is significantly higher than the  $K_{\rm M}$  value (~100  $\mu{\rm M}$ ), to determine the catalytic properties of the demethylases solely dependent on the cofactor analogues.<sup>29,30</sup>

Analysis of the kinetic parameters revealed that F185G-ethyl  $\alpha$ KG possessed the strongest catalytic prowess and is only 5-fold weaker than the wildtype system (Figures 4B,C, S21–S26). Allyl  $\alpha$ KG 3 was next in the series, and its binding to the mutant appeared to be the main contributing factor as evident from the  $K_{\rm M}$  value. A majority of the cofactor derivatives showed comparable binding aptitude toward their cognate

mutant that paralleled that of the corresponding wild type pair, indicating that steric complementarity plays a critical role in the binding of cofactor analogues during catalysis. Thus, the overall lower turnover  $(k_{cat})$  for the engineered pairs is likely due to a compromised transition-state structure and product release, or a combination of both. We observed that within the series of the cofactor analogues, propargyl  $\alpha$ KG 4 showed weaker efficiency, presumably due to a bulky ethynyl moiety affecting some or all of the catalytic steps. It is worth noting that the  $\alpha KG$  analogues were prepared as racemic mixtures, and thus the  $K_{\rm M}$  values could be improved further with enantiomerically enriched cofactors. Taken together, the KDM4A-F185G mutant and selected αKG analogues displayed varied but robust catalytic proficiency in demethylating the substrate peptide and are thus suitable for rapidly demethylating cognate substrate in an orthogonal manner.

Establishing Orthogonality of  $\alpha$ KG Analogues. We next sought to examine the abiotic cofactors for their specificity toward a panel of human  $\alpha$ KG-dependent dioxygenases. We expressed and purified catalytic domains of KDM6B, TET2-3, and ALKBH9 (FTO): these proteins represent histone, DNA, and RNA demethylases, respectively.<sup>31–34</sup> The catalytic activity of the enzymes was assessed using synthesized peptide or nucleic acid substrates and analyzed by MALDI-TOF MS (Figures 4D, S27-S30). All four demethylases showed robust activity on their cognate substrates in the presence of canonical cofactor aKG, confirming their biochemical integrity. However, the representative bulky  $\alpha KG$  analogues 2-9 failed to stimulate oxygenase activity of the enzymes at 100  $\mu M$ concentration that was sufficient to achieve 100% activity for the mutants. Taken together, our biochemical results on a total of nine wild-type demethylases (KDM4A-E, KDM6B, TET2 and 3, and FTO) with varied substrate scope and catalytic mechanisms strongly argue for the orthogonality of the  $\alpha$ KG analogues.

To further examine the orthogonality of the analogues, we performed a systematic cofactor competition experiment. Wildtype KDM4A was incubated with varying concentrations of ethyl  $\alpha$ KG followed by activation with the natural cofactor

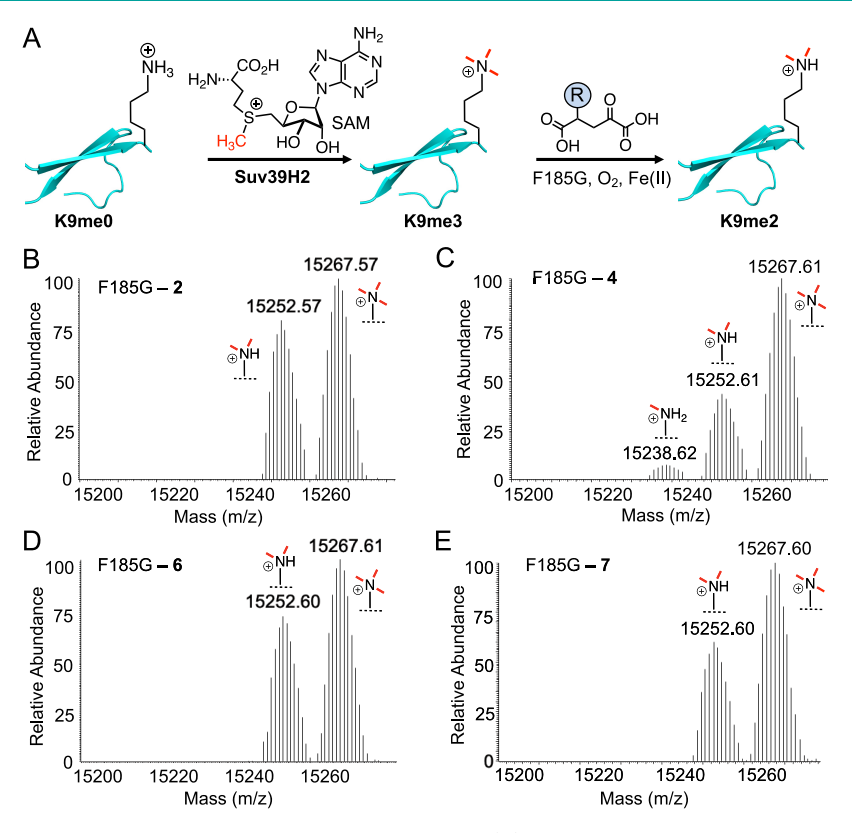
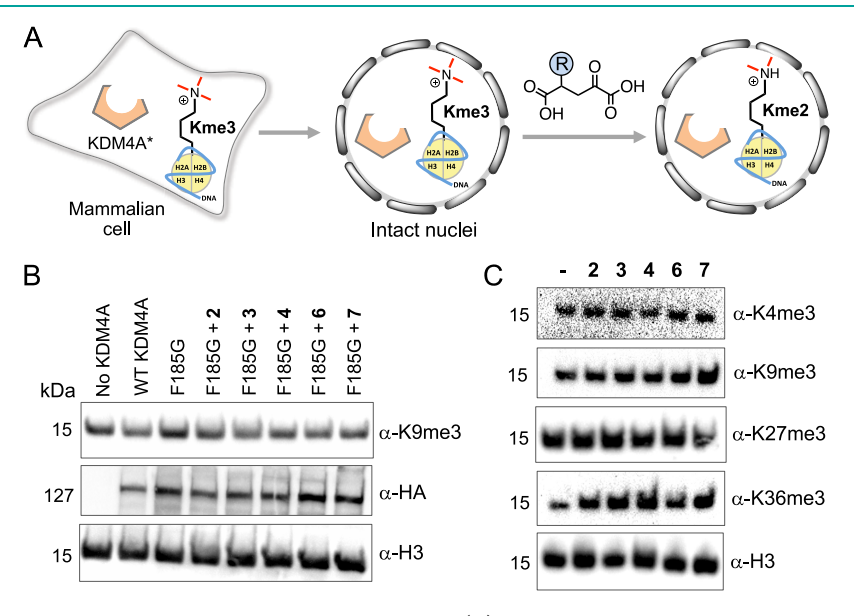


Figure 5. Activity of as KDM4A $-\alpha$ KG analogues on full-length histone H3. (A) Biochemical steps showing tandem activity of SUV39H2 to generate H3K9me3 followed by demethylation to H3K9me2 by the as pairs. (B-E) Deconvoluted ESI LC-MS spectra of histone demethylation by the indicated as pairs.



**Figure 6.** Activity of *as* KDM4A $-\alpha$ KG analogues on nuclear histone H3. (A) Schematic showing steps to examine the activity of engineered enzyme-cofactor pairs on nuclear H3. (B) Analogue-sensitive activation of KDM4A: nuclear histones can be demethylated using F185G and selected cofactor analogues at varying degrees as determined by Western blot with appropriate antibodies (lanes 4-8). Endogenous  $\alpha$ KG activated wild type KDM4A but not the mutant (lanes 2 and 3). (C) Selected set of  $\alpha$ KG derivatives did not change the level of key methylation sites (H3K4me3, H3K9me3, H3K27me3, and H3K36me3) on the nuclear histone, demonstrating their inertness toward endogenous wildtype human KDMs.

 $\alpha$ KG. No noticeable inhibition of wildtype KMD4A activity by the ethyl analogue was observed (Figure S31). In a reverse competition experiment, we also noticed that  $\alpha$ KG did not show any inhibitory effects on the F185G-ethyl  $\alpha$ KG system (Figure S32). These studies further demonstrate a mutual

orthogonality between the wildtype and engineered demethylases and their cognate cofactors.

Demethylation of Full-Length Histone H3 by Engineered KDM4A. Degree-specific lysine methylation on full-length substrate proteins is carefully regulated by reverse-acting

methyltransferases (KMTs) and demethylases (KDMs). For example, dynamic H3K9 methylation-demethylation is achieved by the sequential activity of a multimeric complex of KMTs (G9a, GLP1, Suv39H1/2, SETDB1) and diverse KDMs (KDM4A-E).<sup>35,36</sup> To demonstrate that the engineered KDM4 can act in tandem with KMT on full-length histone H3, we set up an in vitro methylation-demethylation assay (Figure 5A). Bacterially expressed H3 was subjected to methylation using the catalytic domain of Suv39H2 and S-adenosylmethionine (SAM), a universal methyl donor.<sup>37</sup> An efficient methylation (H3K9me3) level was confirmed using ESI LC-MS only in Suv39H2 and SAM-treated samples, and not in control samples lacking either component (Suv39H2 or SAM; Figure S33). In an in situ demethylation assay, incubation with the KDM4A-F185G mutant and a selected  $\alpha$ KG analogue (2, 4, 6, or 7), resulted in the formation of H3K9me2 as detected by mass spectrometry (Figure 5B-E). Di- and monomethylated H3 was undetectable when the analogue-sensitive mutant was incubated with the canonical  $\alpha KG$  1. These results recapitulate the tandem KMT-KDM activity that occurs in certain loci in the genome and further demonstrate that engineered demethylase along with its cognate cofactor can control the dynamic methylation status on full-length substrates.

Demethylation of Nuclear Histone by KDM4A Variant. Finally, we sought to examine the ability of the abiotic cofactors to activate the analogue-sensitive KDM4A variant in a cellular environment, which also harbors >60 endogenous αKG-dependent enzymes.<sup>38</sup> Given that KDMs carry multiple domains that regulate member-specific genome localization and substrate demethylation (Figure S2), we generated an F185G mutant in full-length human KDM4A. Upon transient expression of the mutant in HEK293T cells, intact nuclei were isolated and subjected to demethylation of chromosomal histones by treatment with  $\alpha$ KG analogues (Figure 6A). Given that all of the components of chromatin and associated enzymes are localized in the nucleus, isolated nuclei offer a physiologically relevant substrate to directly test the effect of  $\alpha KG$  and its analogues, which have limited cell permeability. 39,40 To gauge the extent of lysine demethylation, the H3K9me3 level was analyzed by Western blot using a corresponding antibody (Figure 6B). While wild type KDM4A demonstrated robust demethylation with endogenous  $\alpha KG$ , the mutant failed to mediate any noticeable demethylation, as no difference in H3K9me3 was observed when compared to nontransfected cells, consolidating the orthogonality of the engineered variant. However, H3K9me3 demethylation ensued when nuclei expressing the F185G mutant were treated with the cofactor analogues. Ethyl (2), allyl (3), and isobutyl (6)  $\alpha$ KG analogues led to robust demethylation of nuclear histone H3, mirroring their in vitro catalytic efficacy. This result demonstrates that enzymatic activation of an otherwise inactive KDM4 variant in the cellular milieu is indeed attainable by paired cofactors. Furthermore, ethyl  $\alpha$ KG led to a graded decrease in H3K9me3 level in a dose-response manner, demonstrating a tunable activation of histone demethylases using an abiotic cofactor (Figure S34).

We next performed a cofactor competition experiment in isolated nuclei expressing either wildtype or full-length mutant protein. The natural cofactor and its ethyl derivative remained refractory (neither activating or inhibitory) toward the engineered and wildtype KDM4A, respectively, further confirming a mutual orthogonality of the demethylase systems

(Figure S34). Finally, we examined the off-target activity of the  $\alpha$ KG analogues on endogenous histone demethylases (Figure 6C). Isolated nuclei from nontransfected cells were treated with 100  $\mu$ M of 2–9 and analyzed for key methylated lysine sites in H3 (H3K4me3, H3K9me3, H3K27me3, and H3K36me3). Upon comparison with untreated cells, no noticeable changes in lysine methylation levels were observed at these sites. This result further confirms the inertness of the bulky  $\alpha$ KG derivatives toward more than 20 human KDMs that act on H3 and their selectivity toward the analogue-sensitive demethylase variants.

#### CONCLUSIONS

Biochemical degeneracy of enzymes imparted by commonness in fold, cofactor and catalytic mechanism constitutes a major barrier in elucidating member-specific protein function. More than 30 human KDMs along with other  $\alpha$ KG-dependent enzymes pose the same challenge in developing isoformspecific small-molecule probes to unravel their functions with temporal control. In this work, we explored an analoguesensitive "chemical rescue" strategy to resurrect an inactive KDM mutant to perform native-like functions. The rationale for such conditional enzyme activation lies in establishing, rather than abolishing, degree-specific methylation patterns by a given KDM in chromosomal histones. On the basis of our in vitro study, we identified a conserved phenylalanine which acts as a gatekeeper residue in the KDM4 subfamily. A spacecreating point mutation at this site rendered the mutant ineffective toward canonical aKG, reminiscent of pharmacological and genetic perturbations. However, abiotic cofactors carrying complementary steric appendages could sensitize the "dead" mutants to restore demethylase activity, thus offering a powerful tool for probing the biological function of degreespecific lysine demethylation. The  $\alpha KG$  analogues do not interfere with the native KDM4s and other  $\alpha$ KG-dependent enzymes likely due to steric clash with the conserved gatekeeper residue and hence can serve as chemical probes for a specific allele. Given that the human genome rarely encodes such analogue sensitive KDMs, the engineered system is expected to be highly orthogonal across the KDM superfamily. Detailed steady-state kinetic experiments showed that the mutant-cofactor pairs are catalytically competent and comparable to the wild type demethylases. Furthermore, the engineered KDM4 was shown to act in tandem with histone methyltransferase to modulate lysine methylation in full-length histones. Finally, the  $\alpha$ KG analogues activated the full-length analogue-sensitive variant expressed in cultured human cells to modulate the catalytic activity of a specific KDM4 allele on chromosomal histones. Future experiments would involve knock-in of KDM4 variants into the endogenous locus using genome-editing tools for temporal manipulation of demethylase members with cell-permeable aKG analogues. Furthermore, we predict extending the engineering platform to other members of the aKG-dependent dioxygenase superfamily, which are beginning to emerge as critical regulators of mammalian gene expression.

# METHODS

General Synthetic Methods toward  $\alpha$ KG Analogues 2–9. General Method for Alkylation Step. 2,2-Dimethoxyglutaric acid (1 equiv) was dissolved in THF and then cooled to -78 °C. A 1 M solution of lithium bis(trimethylsilyl)amide in THF (1.2 equiv) was added dropwise over 10 min. The reaction mixture was stirred at -78

 $^{\circ}$ C for 1 h. Next, R-Br, where R = alkyl, alkenyl, alkynyl, or aryl, was added dropwise. The reaction was stirred overnight and allowed to reach RT. The reaction was quenched by the addition of 10 mL of saturated NH<sub>4</sub>Cl solution. The product was extracted with 20 mL of ethyl acetate (three times). The organic layers were combined, dried with Na<sub>2</sub>SO<sub>4</sub>, concentrated under reduced pressure, and purified via flash chromatography using EtOAc—hexanes solvent system from 1:9–2:8.

General Method for Catalytic Hydrogenation. The protected and alkylated products 15–19 were stirred to dissolve in 4 mL of ethyl acetate, then Pd/C (10 mol % Pd) was added and the reaction was degassed under a vacuum. A hydrogen balloon was connected to the reaction flask, and the reaction was stirred at RT overnight. The reaction was filtered through Celite and concentrated under reduced pressure. The product was purified via flash chromatography with an EtOAc—hexanes solvent system 1:8.

General Method for Deketalization. The fully protected and alkylated product was dissolved by stirring in 1 mL of dichloromethane. To the stirring solution, 0.1 mL of water and 1 mL of trifluoroacetic acid were added. The reaction mixture was stirred at RT for 2 h. The reaction was neutralized then concentrated under reduced pressure and purified by flash chromatography using an EtOAc—hexanes solvent system generally at 1:5.

General Method for Ester Hydrolysis and HPLC Purification. Last, 1 equiv of dimethyl ester compounds was dissolved in MeOH/H<sub>2</sub>O (1.2:0.8 mL). Solid LiOH (2.5 equiv) was added to the reaction and stirred at RT for 2 h. The reaction was monitored with TLC. The reaction was quenched and neutralized with the addition of 1 N HCl. Methanol was removed from the compound under reduced pressure. The compound was diluted with 1 mL of water and filtered through a 0.2  $\mu$ m filter. The final product was obtained through HPLC purification using a C18 column (Waters XBridge) and the following method: solvent A = water; solvent B = acetonitrile; method 0 min, 5% B; 20 min, 50% B; 25 min, 95% B; with a flow rate of 4 mL/min and UV was monitored at 210 nm. The purest fractions were collected and concentrated first under speedvac to remove acetonitrile via lyophilization. The syntheses of  $\alpha$ KG analogues 2 and 6 are previously reported. 14

**Synthesis and Purification of Peptides.** Peptides were synthesized by the University of Pittsburgh Peptide Synthesis Facility (Table S4). The Peptide Synthesis facility desalted and sent crude peptides for further purification. Crude peptides were reverse phase HPLC purified on a Waters XBridge Prep C18 column with the following method: solvent A = 0.1% trifluoroacetic acid,  $H_2O$ ; solvent B = acetonitrile, 0 min, 5% B; 10 min, 55% B; 12 min, 95% B at 4 mL/min monitoring UV at 205 nm. The column was thoroughly washed with 100% acetonitrile between runs, then equilibrated back to starting conditions for 5 min. The purest fractions were collected and concentrated first under speedvac to remove acetonitrile via lyophilization. The peptides were reconstituted in  $H_2O$ , and concentrations were calculated from absorbance at 205 nm ( $A_{205}$ , taken  $\varepsilon_{205} = 30$  L/(g cm)). MALDI-TOF of the final product confirmed the purity of the peptide.

Synthesis and Purification of Oligonucleotides. The oligonucleotides (Table S4) were synthesized using standard phosphoramidite monomers obtained from Glen Research using 1H-tetrazole as an activator reagent in an Expedite Nucleic Acid Synthesis System (PerSeptive Biosystems) with DMT-ON protocol. 5mC and m6A phosphoramidites were purchased from Glen Research. Elongated (5 min for DNA and 30 min for RNA) coupling times were used for the modified bases; for the standard bases, normal (2 min for DNA and 13 min for RNA) coupling times were applied. The DNA oligo was resuspended and incubated in ammonium hydroxide (33% v/v) for 24 h at RT to cleave the oligo from solid support and to deprotect the bases. The RNA oligo was cleaved from the solid support using a 1:1 mixture of ammonium hydroxide and methylamine (AMA); base deprotection was carried out by incubating this mixture at 65 °C for 10 min. For TBDMS deprotection, the AMA was first evaporated via Speedvac, and the oligo was resuspended in 115  $\mu$ L of DMSO. Then, 60  $\mu$ L of

trimethylamine and 75  $\mu$ L of trimethylamine-hydrofluoric acid were added, and the solution was incubated for 2.5 h at 65 °C. The oligo was quenched with RNA quenching buffer (Glen Research) and purified via a Glen Pak purification cartridge according to the manufacturer's protocol. The elution buffer was evaporated, and the oligo was resuspended in nuclease free water. Purity was checked with MALDI, and no further purification steps were necessary. For DNA oligonucleotides, preliminary purification and DMT deprotection were carried out using a Poly Pak<sup>II</sup> purification cartridge (Glen Research) according to the standard protocol provided by the manufacturer. Crude DNA oligonucleotides were purified by HPLC using a C-18 column (solvent A, 0.1 M TEAA; solvent B, acetonitrile; gradient for DNA, 0 min, 5% B; 10 min, 40% B; 15 min, 100% B with a flow rate 4 mL/min; gradient for RNA, 0 min, 3% B; 20 min, 15% B; 25 min, 100% B with a flow rate 4 mL/min). The fractions were collected and concentrated with a SpeedVac concentrator followed by lyophilization and redissolved in RNAase free water. The quality and purity of synthesized DNA and RNA was monitored by MALDI-TOF-MS.

Mutagenesis, Expression, and Purification of  $\alpha$ KG-Dependent Dioxygenases. The N-terminal 6xHis-tagged human KDM4A-jmjC domain (catalytic domain of KDM4A) bacterial expression construct pNIC28-Bsa4 was obtained from Addgene (ID: 38846). The expression and purification of the wild type enzyme and the mutant generation followed the method reported earlier. <sup>14</sup>

The bacterial expression constructs carrying N-terminal streptagged catalytic domains of human KDM4B and KDM4D jmjC were kindly provided by Prof. Raymond Trievel, University of Michigan. <sup>22,30</sup> The expression and purification of the wild type enzyme and the mutant generation followed by expression and purification were reported earlier. <sup>14</sup>

The N-terminal 6xHis-tagged human KDM4C catalytic domain construct for bacterial expression was a kind gift from Prof. Danica Fujimori, UCSF. The resulting expression and purification of the wild type enzyme and the mutant generation followed by expression and purification were reported earlier. <sup>14</sup>

The N-terminal 6xHis-tagged KDM4E construct for bacterial expression was purchased from Addgene (#38990). The wild type KDM4E plasmid was transformed into E. coli BL21 (DE3) competent cells (Invitrogen) using the pNIC28-Bsa4 kanamycin-resistant vector. A single colony was grown overnight at 37 °C in 10 mL of Luria-Bertani (LB) broth in the presence of 50  $\mu$ g/mL of kanamycin and 35  $\mu$ g/mL of chloramphenicol. The culture was diluted 100-fold and allowed to grow at 37 °C to an optical density (OD<sub>600</sub>) of 0.8, and protein expression was induced overnight at 17  $^{\circ}\text{C}$  with 1 mM IPTG in an Innova 44 Incubator shaker (New Brunswick Scientific). KDM4E was purified from pelleted cells by resuspending in lysis buffer (50 mM Tris-HCl, pH 8.0, 200 mM NaCl, 5 mM  $\beta$ -ME, 10% glycerol, 25 mM imidazole, lysozyme, Dase, and Pierce protease inhibitor cocktail). The cells were lysed by sonication at 60 mA for 10 s on followed by 10 s off, for a total of 2 min. The cell debris was pelleted at 13 000 rpm for 40 min. The soluble cell extracts were incubated with Ni-NTA agarose resin (Thermo) according to the manufacturer's protocol. Beads were washed with 20 column volumes of was buffer (50 mM Tris-HCl at pH 8.0, 200 mM NaCl, 10% glycerol 5 mM  $\beta$ -ME, and 25 mM imidazole). Proteins were eluted with five column volumes of elution buffer (50 mM Tris at pH 8.0, 200 mM NaCl, 5 mM  $\beta$ -ME, 10% glycerol, and 400 mM imidazole). Proteins were next purified via size exclusion chromatography on an AKTA pure FPLC system with 50 mM of Tris at pH 8.0, 200 mM NaCl, and 10% glycerol. Fractions with pure protein were combined and concentrated using a Sartorius Vivaspin 10 kDa centrifugal concentrator. Bradford Dye (BioRad) was used to quantify the protein concentration using BSA as a standard. The concentrated proteins were aliquoted, flash frozen, and stored at -80 °C until use. KDM4E variant F186G was generated using a QuikChange Lightening site-directed mutagenesis kit (Agilent Technologies). The resulting mutant plasmid was confirmed by DNA sequencing, and the variant was expressed and purified as above.

The plasmid constructs for the catalytic domain of KDM6B was kindly provided by Prof. Christopher Schofield of the University of Oxford. The resulting expression and purification of the wild type enzyme was reported earlier. 14

The plasmids for the catalytic domain of the m<sup>6</sup>A-RNA demethylase FTO and 5mC demethylases TET2–3 were kind gifts from Profs. Chuan He of the University of Chicago and Yanhui Xu of the Fudan University, respectively.<sup>34,33</sup> Wild type FTO and TETs and were expressed and purified as stated earlier for N-6xHis tag proteins.<sup>42,43</sup>

**Expression and Purification of Formaldehyde Dehydrogenase (FDH).** The bacterial expression construct of N-terminal 6xHistagged *P. putida* FDH in pET28 vector was obtained from the Bhagwat laboratory at the Wayne State University. The resulting expression and purification of the wild type enzyme and the mutant generation followed by expression and purification were reported earlier. The provided that the state of the provided that the state of the provided that the provided

**Expression and Purification of SUV39H2.** SUV39H2 for bacterial expression in pET28a vector was obtained from Prof. Minkui Luo at the Sloan-Kettering Institute. The protein was expressed and purified as reported earlier.<sup>37</sup>

**Expression and Purification of Histone H3.** Gene sequence encoding wild type *Xenopus laevis* histone H3 was a kind gift from Prof. Minkui Luo at the Memorial Sloan-Kettering Cancer Center. The resulting expression and purification of the protein were reported earlier. <sup>14</sup>

MALDI Demethylase Activity Assay. As a measure of enzymatic activity, an in vitro demethylase assay was employed followed by MALDI-TOF for product observation. 14,30 Each histone demethylase assay sample included 10  $\mu$ M enzyme, 10  $\mu$ M peptide, 100  $\mu$ M  $\alpha$ KG/ analogues, 50 mM Tris at pH 8, 100 µM freshly prepared (NH<sub>4</sub>)<sub>2</sub>Fe(SO<sub>4</sub>)<sub>2</sub>, and 2 mM freshly prepared L-ascorbic acid with a total assay volume of 10 µL. Assay components were aliquoted and the reaction was started by the addition of  $\alpha KG$  analogues followed by brief centrifugation and incubation at 37 °C for 30 min. One microliter of the assay sample was mixed with 1  $\mu$ L of  $\alpha$ -cyano-4hydroxycinnamic acid matrix (dissolved in 1:1 ratio of 0.1% TFA H<sub>2</sub>O/acetonitrile) directly on the MALDI plate. The sample was ionized with Bruker FlexControl in the reflectron positive mode and analyzed on Bruker FlexAnalysis software. The percent demethylated peptide was calculated by first multiplying the K9me1 peak by 2 and the K9me0 peak by 3 to account for the multiple demethylation events on the peptide. The percent peak area was calculated, and the K9me2, me1, and me0 peaks were summed to give the relative percent of demethylated peptide. A negative control was provided for each assay, which included all components of the assay except for  $\alpha$ KG.

For DNA demethylation, each assay sample included 10  $\mu$ M double-stranded DNA (5′-CAC-5<sup>m</sup>C-GGTG-3′), 50 mM HEPES at pH 8, 100 mM NaCl, 100  $\mu$ M (NH<sub>4</sub>)<sub>2</sub>Fe(SO<sub>4</sub>)<sub>2</sub>, 2 mM L-ascorbic acid, 1 mM DTT (prepared freshly), 1 mM ATP, 10  $\mu$ M TET2, and 100 mM Cofactors 1–9.<sup>33,44</sup> The samples were incubated for 3 h at 37 °C. The TET3 assay was done similarly, but 500 mM  $\alpha$ KG 1–9 was used. The samples were desalted using BT AG50W-X8 Resin (BioRad, Cat # 143–5441). The DNA was analyzed via MALDI-TOF in the reflectron negative mode using a 3-hydroxypicolinic acid (3-HPA) matrix with ammonium citrate 1:9 (dissolved in a 1:1 mixture of 0.1% TFA:Acetonitrile); a similar percentage product was calculated by the procedure listed above. A negative control was provided for each assay, which included all components of the assay except for  $\alpha$ KG.

For mRNA demethylation by FTO, each assay sample included 10  $\mu$ M RNA synthesized to contain a full phosphorothioate backbone with a methylated adenosine residue (m<sup>6</sup>A) (5'-CUG-G-m<sup>6</sup>A-CUG-G-3'), 50 mM HEPES at pH 8.0, 150 mM KCl, 75  $\mu$ M (NH<sub>4</sub>)<sub>2</sub>Fe(SO<sub>4</sub>)<sub>2</sub>, 2 mM L-ascorbic acid, 10  $\mu$ M FTO, and 100  $\mu$ M cofactors 1–9.<sup>34</sup> After addition of the  $\alpha$ KG analogues, the samples were incubated at 37 °C for 30 min, and they were subsequently quenched with 7.5 mM EDTA. The samples were prepared for the MALDI-TOF readout by first incubating with AG50W-X8 desalting

resin and then spotted onto the MALDI plate with 2',4',6'-trihydroxyacetophenone monohydrate and ammonium citrate 1:9 (dissolved in a 1:1 mixture of 0.1% TFA/acetonitrile). Percent demethylated oligonucleotide was calculated by summing the percent peak area of the demethylated oligo and the formylated adenosine oligo peak. A negative control was provided for each assay, which included all components of the assay except for  $\alpha$ KG.

Coupled Fluorescence Assay. The catalytic efficiency of the KDM4A WT and F185G mutant to  $\alpha$ KG and the analogues was determined by employing a coupled fluorescence assay. The formaldehyde product of the demethylase assay was used as a cofactor for FDH to reduce NAD+ to NADH, and the fluorescence of NADH at 490 nm was monitored to calculate the amount of NADH produced.<sup>28,30</sup> The assay components were split into an enzyme cocktail (containg 50 mM HEPES at pH 8.0, 100  $\mu$ M (NH<sub>4</sub>)<sub>2</sub>Fe- $(SO4)_2$ , 2 mM L-ascorbic acid, 200 nM FDH, and 1  $\mu$ M KDM4A WT or F185A) and a substrate cocktail (0-250  $\mu$ M  $\alpha$ KG (1-4 and 6-7), 1 mM NAD+, and 300  $\mu$ M H3K9me3 peptide). The enzyme cocktail was applied to a 384-well white Corning plate followed by the enzyme cocktail. The plate was briefly centrifuged, and the accumulation of NADH was monitored on a TECAN Infinite M1000Pro plate reader (excitation = 340 nm, emission = 490 nm). The amount of NADH produced was converted to micromolar H3K9me3, demethylated using the NADH calibration curve. The initial rates of the reaction were determined by plotting the data within the linear range on GraphPad Prism software. The slopes of the reaction were fitted to the Michaelis-Menten equation to determine the  $K_{\rm M}$  and  $k_{\rm cat}$  values. These experiments were performed in duplicate.

**NADH Calibration Curve.** A NADH calibration curve was generated to convert the fluorescence signal to the amount of NADH present. Then, using the reaction stoichiometry of 1:1:1 for [NADH]/[formaldehyde]/[H3K9me3], the amount of demethylated peptide can be calculated. NADH (ACROS, cat #124530050) was added to the assay buffer in varying concentrations  $(1-10 \,\mu\text{M})$ . The assay buffer consisted of 50 mM HEPES at pH 8.0, 100  $\mu$ M (NH<sub>4</sub>)<sub>2</sub>Fe(SO<sub>4</sub>)<sub>2</sub>, 2 mM L-ascorbic acid, 1 mM NAD+, 200 nm FDH, and 1  $\mu$ M KDM4A. The assay was loaded onto a 384-well white Corning plate in triplicate, and fluorescence intensity was read by a TECAN Infinite M1000Pro plate reader (excitation = 340 nm, emission = 490 nm).

Tandem Methylation-Demethylation on Full-Length Histone H3 and LCMS Analysis. Recombinant full-length H3 was first trimethylated by SUV39H2. Each reaction mixture contained 2  $\mu M$ SUV39H2, 100  $\mu$ M SAM, 20  $\mu$ M H3, and tris at pH 8.0. SUVH39H2 trimethylated H3K9 in 5 min at RT, afterward SUV39H2 was quenched with 2.5  $\mu M$  small-molecule HMTase Inhibitor II and chaetocin (EMD Millipore, #382191). 45 Demethylation of full length H3K9me3 was immediately carried out with the KDM4A assay. To each reaction tube,  $100 \,\mu\mathrm{M}$  Fe(NH<sub>4</sub>)<sub>2</sub>(SO<sub>4</sub>)<sub>2</sub>, 1 mM ascorbic acid, 40  $\mu$ M KDM4A F185G, and 1 mM  $\alpha$ KG analogue were added, and the assay was incubated at 37 °C for 1 h. The reaction was stopped by placing the tubes on ice, and samples were submitted for LCMS. Sample separation was performed by a Thermo Scientific Dionex UltiMate 3000 UHPLC+ with a Thermo ProSwift RP-2H analytical  $4.6 \times 50$  mm SS column using a multistep gradient with a flow rate of 0.2 mL/min and mobile phases A, 0.1% formic acid in HPLC grade H<sub>2</sub>O, and B, 0.1% formic acid in HPLC grade acetonitrile (method: 0 min, 10% B; 1 min, 10% B; 21 min, 50% B; 22 min, 80% B, then equilibrated back to 10% B). Samples were ionized using electrospray ionization in positive mode, and ions were detected in Thermo Scientific Q-exactive Orbitrap. Xcaliber 2.1 software was used to analyze samples.

Demethylase Activity Assay on Isolated Nuclei. KDM4A mammalian expression plasmid in the CMV vector was purchased from addgene (plasmid #24180). The KDM4A F185G mutant was generated using a Quikchange Lightening Mutagenesis Kit (Agilent) according to the manufacturer's protocol. HEK293T/17 cells (ATCC) were grown in Delbucco's Modified Eagle Medium (DMEM; Corning) with 10% FBS at 37 °C, 5% CO<sub>2</sub>, and 95% relative humidity. When cells reached 80% confluency, 5 µg of

plasmid and 10  $\mu$ g of lipofectamine 2000 (Invitrogen) were incubated with 500 µL of Optimem (Gibco); after 5 min, the plasmid and lipofectamine were combined and incubated at RT for 20 min. The media were changed, and 1 mL of Optimem was added to the flask. Cells were returned to the incubator to grow for 24 h. The media were removed, and cells were washed with ice cold PBS (Corning), then trypsinized with TrpLE Express (Gibco). The trypsinization reaction was quenched with DMEM 10% FBS, and cells were pelleted and then washed once with ice cold PBS. The nuclei were immediately isolated; cells were resuspended in 500  $\mu$ L of nuclear isolation buffer (15 mM Tris at pH 7.5, 60 mM KCl, 15 mM NaCl, 5 mM MgCl<sub>2</sub>, 1 mM CaCl<sub>2</sub>, 1 mM DTT, 2 mM sodium vanadate, 1 mM PMSF, 250 mM sucrose, 1 × Pierce protease inhibitor, and 0.3% NP40). Cells were incubated on ice for 5 min, then nuclei were pelleted at 2000g for 5 min at 4 °C. The nuclear pellet was resuspended in 100  $\mu$ L of assay buffer (50 mM Tris at pH 8.0, 100  $\mu$ M (NH<sub>4</sub>)<sub>2</sub>Fe(SO<sub>4</sub>)<sub>2</sub>, 2 mM ascorbic acid, 1 mM PMSF, and 1 × Pierce protease inhibitor). Ten microliters of the isolated nuclei were aliquoted and incubated with 100  $\mu$ M cofactors 2, 3, 4, 6, and 7 for 1 h at 37 °C with gentle shaking (300 rpm). The nuclei were lysed by adding 0.2% NP40 and sonicating in a water bath (Q-sonica) for 5 min. Nuclear debris were pelleted at 2000g for 5 min at 4 °C. The nuclear extracts were quantified with Bradford assay (Bio-Rad laboratories) using BSA as a standard. Trimethylated histone levels were analyzed by Western blotting with 30  $\mu$ g of nuclear extracts.

Western Blotting. Nuclear extracts were separated on SDS-PAGE and transferred onto a 0.2 mm supported nitrocellulose membrane via a semidry blotting apparatus (Bio-Rad Laboratories) at a constant voltage of 15 V for 30 min or via a wet blotting tank at 80 V for 1 h. Membranes were blocked with 5% Bovine Serum Albumin (BSA) in TBST buffer (50 mM Tris HCl at pH 7.6, 200 mM NaCl, 0.1% Tween 20) for 1 h at RT with gentle shaking. The blocking buffer was removed, and membranes were washed with TBST. Immunoblotting was performed with diluted primary antibodies (H3K4me3, cat #9751S, H3K9me3, cat #13969S, H3K36me3 cat #4909S, HA cat #3724S, histone H3 as loading control cat # 9715, in a 1:1000 dilution from Cell Signaling Technology; host rabbit and H3K27me3, cat #GTX50901, in a 1:400 dilution from GeneTex; host mouse) at 4 °C overnight with gentle shaking. The antibody solution was removed, and the membranes were washed with TBST three times for 5 min each, then incubated with 1:5000 dilute HRP-conjugated secondary antibody goat anti-rabbit IgG (cat #7040 Cell Signaling Technology) or goat anti-mouse IgG (cat #7076 Cell Signaling Technology) for 2 h at RT. To remove the secondary antibodies, the membrane was washed with TBST three times, 5 min each. Subsequently, the membrane was incubated with Pierce ECL Western Blotting Substrate (ThermoScientific cat # PI32160) following the manufacturer's protocol. The membrane was imaged on BioRad chemidoc and analyzed with BioRad Image Lab software.

#### ASSOCIATED CONTENT

# Supporting Information

The Supporting Information is available free of charge at https://pubs.acs.org/doi/10.1021/acschembio.1c00335.

Synthetic schemes, characterization data of the  $\alpha$ KG analogues, enzyme assay data, mass spectrometry data,  $^{1}$ H and  $^{13}$ C NMR spectra of the  $\alpha$ KG analogues and the relevant intermediates (PDF)

# AUTHOR INFORMATION

# **Corresponding Author**

Kabirul Islam — Department of Chemistry, University of Pittsburgh, Pittsburgh, Pennsylvania 15260, United States; orcid.org/0000-0002-8680-6130; Email: kai27@pitt.edu

#### **Authors**

Valerie Scott — Department of Chemistry, University of Pittsburgh, Pittsburgh, Pennsylvania 15260, United States Debasis Dey — Department of Chemistry, University of Pittsburgh, Pittsburgh, Pennsylvania 15260, United States; orcid.org/0000-0002-3612-860X

Jordan Kuwik – Department of Chemistry, University of Pittsburgh, Pittsburgh, Pennsylvania 15260, United States Kathryn Hinkelman – Department of Chemistry, University of Pittsburgh, Pittsburgh, Pennsylvania 15260, United States Megan Waldman – Department of Chemistry, University of Pittsburgh, Pittsburgh, Pennsylvania 15260, United States

Complete contact information is available at: https://pubs.acs.org/10.1021/acschembio.1c00335

#### Notes

The authors declare no competing financial interest.

#### ACKNOWLEDGMENTS

We thank the University of Pittsburgh, the National Science Foundation (MCB-1817692), and the National Institutes of Health (R01GM123234, R01GM130752) for financial support; S. Sappa for reagents; and D. Chakraborty and members of our laboratory for editing of the manuscript.

# REFERENCES

- (1) Kooistra, S. M.; Helin, K. Molecular mechanisms and potential functions of histone demethylases. *Nat. Rev. Mol. Cell Biol.* **2012**, *13* (5), 297–311.
- (2) Mosammaparast, N.; Shi, Y. Reversal of histone methylation: biochemical and molecular mechanisms of histone demethylases. *Annu. Rev. Biochem.* **2010**, *79*, 155–79.
- (3) Whetstine, J. R.; Nottke, A.; Lan, F.; Huarte, M.; Smolikov, S.; Chen, Z.; Spooner, E.; Li, E.; Zhang, G.; Colaiacovo, M.; Shi, Y. Reversal of histone lysine trimethylation by the JMJD2 family of histone demethylases. *Cell* **2006**, *125* (3), 467–81.
- (4) Guerra-Calderas, L.; Gonzalez-Barrios, R.; Herrera, L. A.; Cantu de Leon, D.; Soto-Reyes, E. The role of the histone demethylase KDM4A in cancer. *Cancer Genet.* **2015**, 208 (5), 215–224.
- (5) Das, P. P.; Shao, Z.; Beyaz, S.; Apostolou, E.; Pinello, L.; De Los Angeles, A.; O'Brien, K.; Atsma, J. M.; Fujiwara, Y.; Nguyen, M.; Ljuboja, D.; Guo, G.; Woo, A.; Yuan, G. C.; Onder, T.; Daley, G.; Hochedlinger, K.; Kim, J.; Orkin, S. H. Distinct and combinatorial functions of Jmjd2b/Kdm4b and Jmjd2c/Kdm4c in mouse embryonic stem cell identity. *Mol. Cell* **2014**, *53* (1), 32–48.
- (6) Thinnes, C. C.; England, K. S.; Kawamura, A.; Chowdhury, R.; Schofield, C. J.; Hopkinson, R. J. Targeting histone lysine demethylases progress, challenges, and the future. *Biochim. Biophys. Acta, Gene Regul. Mech.* **2014**, *1839* (12), 1416–32.
- (7) Islam, K. Allele-specific chemical genetics: concept, strategies, and applications. ACS Chem. Biol. 2015, 10 (2), 343-63.
- (8) Islam, K. The Bump-and-Hole Tactic: Expanding the Scope of Chemical Genetics. *Cell chemical biology* **2018**, 25 (10), 1171–1184.
- (9) Hertz, N. T.; Berthet, A.; Sos, M. L.; Thorn, K. S.; Burlingame, A. L.; Nakamura, K.; Shokat, K. M. A neo-substrate that amplifies catalytic activity of parkinson's-disease-related kinase PINK1. *Cell* **2013**, *154* (4), 737–47.
- (10) Guo, Z.; Zhou, D.; Schultz, P. G. Designing small-molecule switches for protein-protein interactions. *Science (Washington, DC, U. S.)* **2000**, 288 (5473), 2042–5.
- (11) Qiao, Y.; Molina, H.; Pandey, A.; Zhang, J.; Cole, P. A. Chemical rescue of a mutant enzyme in living cells. *Science (Washington, DC, U. S.)* **2006**, *311* (5765), 1293–7.
- (12) Deckert, K.; Budiardjo, S. J.; Brunner, L. C.; Lovell, S.; Karanicolas, J. Designing allosteric control into enzymes by chemical rescue of structure. *J. Am. Chem. Soc.* **2012**, *134* (24), 10055–60.

- (13) Lopez, M. S.; Kliegman, J. I.; Shokat, K. M. The logic and design of analog-sensitive kinases and their small molecule inhibitors. *Methods Enzymol.* **2014**, *548*, 189–213.
- (14) Breski, M.; Dey, D.; Obringer, S.; Sudhamalla, B.; Islam, K. Engineering Biological C–H Functionalization Leads to Allele-Specific Regulation of Histone Demethylases. *J. Am. Chem. Soc.* **2016**, *138* (41), 13505–13508.
- (15) Loenarz, C.; Schofield, C. J. Expanding chemical biology of 2-oxoglutarate oxygenases. *Nat. Chem. Biol.* **2008**, *4* (3), 152–6.
- (16) Ng, S. S.; Kavanagh, K. L.; McDonough, M. A.; Butler, D.; Pilka, E. S.; Lienard, B. M.; Bray, J. E.; Savitsky, P.; Gileadi, O.; von Delft, F.; Rose, N. R.; Offer, J.; Scheinost, J. C.; Borowski, T.; Sundstrom, M.; Schofield, C. J.; Oppermann, U. Crystal structures of histone demethylase JMJD2A reveal basis for substrate specificity. *Nature* 2007, 448 (7149), 87–91.
- (17) Labbe, R. M.; Holowatyj, A.; Yang, Z. Q. Histone lysine demethylase (KDM) subfamily 4: structures, functions and therapeutic potential. *Am. J. Transl. Res.* **2013**, *6* (1), 1–15.
- (18) Pack, L. R.; Yamamoto, K. R.; Fujimori, D. G. Opposing Chromatin Signals Direct and Regulate the Activity of Lysine Demethylase 4C (KDM4C). *J. Biol. Chem.* **2016**, 291 (12), 6060–70.
- (19) Lee, J.; Thompson, J. R.; Botuyan, M. V.; Mer, G. Distinct binding modes specify the recognition of methylated histones H3K4 and H4K20 by JMJD2A-tudor. *Nat. Struct. Mol. Biol.* **2008**, *15* (1), 109–11.
- (20) Couture, J. F.; Collazo, E.; Ortiz-Tello, P. A.; Brunzelle, J. S.; Trievel, R. C. Specificity and mechanism of JMJD2A, a trimethyllysine-specific histone demethylase. *Nat. Struct. Mol. Biol.* **2007**, *14* (8), 689–95.
- (21) Wigle, T. J.; Swinger, K. K.; Campbell, J. E.; Scholle, M. D.; Sherrill, J.; Admirand, E. A.; Boriack-Sjodin, P. A.; Kuntz, K. W.; Chesworth, R.; Moyer, M. P.; Scott, M. P.; Copeland, R. A. A High-Throughput Mass Spectrometry Assay Coupled with Redox Activity Testing Reduces Artifacts and False Positives in Lysine Demethylase Screening. *J. Biomol. Screening* **2015**, *20* (6), 810–20.
- (22) Krishnan, S.; Trievel, R. C. Structural and functional analysis of JMJD2D reveals molecular basis for site-specific demethylation among JMJD2 demethylases. *Structure (Oxford, U. K.)* **2013**, *21* (1), 98–108.
- (23) Hillringhaus, L.; Yue, W. W.; Rose, N. R.; Ng, S. S.; Gileadi, C.; Loenarz, C.; Bello, S. H.; Bray, J. E.; Schofield, C. J.; Oppermann, U. Structural and evolutionary basis for the dual substrate selectivity of human KDM4 histone demethylase family. *J. Biol. Chem.* **2011**, 286 (48), 41616–25.
- (24) Zee, B. M.; Levin, R. S.; Dimaggio, P. A.; Garcia, B. A. Global turnover of histone post-translational modifications and variants in human cells. *Epigenet. Chromatin* **2010**, *3* (1), 22.
- (25) Barth, T. K.; Imhof, A. Fast signals and slow marks: the dynamics of histone modifications. *Trends Biochem. Sci.* **2010**, 35 (11), 618–26.
- (26) Ingvarsdottir, K.; Edwards, C.; Lee, M. G.; Lee, J. S.; Schultz, D. C.; Shilatifard, A.; Shiekhattar, R.; Berger, S. L. Histone H3 K4 demethylation during activation and attenuation of GAL1 transcription in Saccharomyces cerevisiae. *Mol. Cell. Biol.* **2007**, 27 (22), 7856–64.
- (27) Radman-Livaja, M.; Liu, C. L.; Friedman, N.; Schreiber, S. L.; Rando, O. J. Replication and active demethylation represent partially overlapping mechanisms for erasure of H3K4me3 in budding yeast. *PLoS Genet.* **2010**, *6* (2), e1000837.
- (28) Roy, T. W.; Bhagwat, A. S. Kinetic studies of Escherichia coli AlkB using a new fluorescence-based assay for DNA demethylation. *Nucleic Acids Res.* **2007**, *35* (21), e147.
- (29) Lohse, B.; Helgstrand, C.; Kristensen, J. B.; Leurs, U.; Cloos, P. A.; Kristensen, J. L.; Clausen, R. P. Posttranslational modifications of the histone 3 tail and their impact on the activity of histone lysine demethylases in vitro. *PLoS One* **2013**, *8* (7), e67653.
- (30) Krishnan, S.; Collazo, E.; Ortiz-Tello, P. A.; Trievel, R. C. Purification and assay protocols for obtaining highly active Jumonji C demethylases. *Anal. Biochem.* **2012**, *420* (1), 48–53.

- (31) Kruidenier, L.; Chung, C. W.; Cheng, Z.; Liddle, J.; Che, K.; Joberty, G.; Bantscheff, M.; Bountra, C.; Bridges, A.; Diallo, H.; Eberhard, D.; Hutchinson, S.; Jones, E.; Katso, R.; Leveridge, M.; Mander, P. K.; Mosley, J.; Ramirez-Molina, C.; Rowland, P.; Schofield, C. J.; Sheppard, R. J.; Smith, J. E.; Swales, C.; Tanner, R.; Thomas, P.; Tumber, A.; Drewes, G.; Oppermann, U.; Patel, D. J.; Lee, K.; Wilson, D. M. A selective jumonji H3K27 demethylase inhibitor modulates the proinflammatory macrophage response. *Nature* 2012, 488 (7411), 404–8.
- (32) Tahiliani, M.; Koh, K. P.; Shen, Y.; Pastor, W. A.; Bandukwala, H.; Brudno, Y.; Agarwal, S.; Iyer, L. M.; Liu, D. R.; Aravind, L.; Rao, A. Conversion of 5-methylcytosine to 5-hydroxymethylcytosine in mammalian DNA by MLL partner TET1. *Science (Washington, DC, U. S.)* 2009, 324 (5929), 930–5.
- (33) Hu, L.; Li, Z.; Cheng, J.; Rao, Q.; Gong, W.; Liu, M.; Shi, Y. G.; Zhu, J.; Wang, P.; Xu, Y. Crystal structure of TET2-DNA complex: insight into TET-mediated 5mC oxidation. *Cell* **2013**, *155* (7), 1545–55
- (34) Fu, Y.; Jia, G.; Pang, X.; Wang, R. N.; Wang, X.; Li, C. J.; Smemo, S.; Dai, Q.; Bailey, K. A.; Nobrega, M. A.; Han, K. L.; Cui, Q.; He, C. FTO-mediated formation of N6-hydroxymethyladenosine and N6-formyladenosine in mammalian RNA. *Nat. Commun.* **2013**, *4*, 1798.
- (35) Fritsch, L.; Robin, P.; Mathieu, J. R.; Souidi, M.; Hinaux, H.; Rougeulle, C.; Harel-Bellan, A.; Ameyar-Zazoua, M.; Ait-Si-Ali, S. A subset of the histone H3 lysine 9 methyltransferases Suv39h1, G9a, GLP, and SETDB1 participate in a multimeric complex. *Mol. Cell* **2010**, *37* (1), 46–56.
- (36) Wu, H.; Min, J.; Lunin, V. V.; Antoshenko, T.; Dombrovski, L.; Zeng, H.; Allali-Hassani, A.; Campagna-Slater, V.; Vedadi, M.; Arrowsmith, C. H.; Plotnikov, A. N.; Schapira, M. Structural biology of human H3K9 methyltransferases. *PLoS One* **2010**, *5* (1), e8570.
- (37) Arora, S.; Horne, W. S.; Islam, K. Engineering Methyllysine Writers and Readers for Allele-Specific Regulation of Protein-Protein Interactions. *J. Am. Chem. Soc.* **2019**, *141* (39), 15466–15470.
- (38) Hausinger, R. P. FeII/alpha-ketoglutarate-dependent hydroxylases and related enzymes. *Crit. Rev. Biochem. Mol. Biol.* **2004**, 39 (1), 21–68.
- (39) Zengeya, T. T.; Kulkarni, R. A.; Meier, J. L. Modular synthesis of cell-permeating 2-ketoglutarate esters. *Org. Lett.* **2015**, *17* (10), 2326–9.
- (40) MacKenzie, E. D.; Selak, M. A.; Tennant, D. A.; Payne, L. J.; Crosby, S.; Frederiksen, C. M.; Watson, D. G.; Gottlieb, E. Cellpermeating alpha-ketoglutarate derivatives alleviate pseudohypoxia in succinate dehydrogenase-deficient cells. *Mol. Cell. Biol.* **2007**, 27 (9), 3282–9.
- (41) Williams, S. T.; Walport, L. J.; Hopkinson, R. J.; Madden, S. K.; Chowdhury, R.; Schofield, C. J.; Kawamura, A. Studies on the catalytic domains of multiple JmjC oxygenases using peptide substrates. *Epigenetics* **2014**, *9* (12), 1596–603.
- (42) Sudhamalla, B.; Wang, S.; Snyder, V.; Kavoosi, S.; Arora, S.; Islam, K. Complementary Steric Engineering at the Protein-Ligand Interface for Analogue-Sensitive TET Oxygenases. *J. Am. Chem. Soc.* **2018**, *140* (32), 10263–10269.
- (43) Hu, L.; Lu, J.; Cheng, J.; Rao, Q.; Li, Z.; Hou, H.; Lou, Z.; Zhang, L.; Li, W.; Gong, W.; Liu, M.; Sun, C.; Yin, X.; Li, J.; Tan, X.; Wang, P.; Wang, Y.; Fang, D.; Cui, Q.; Yang, P.; He, C.; Jiang, H.; Luo, C.; Xu, Y. Structural insight into substrate preference for TET-mediated oxidation. *Nature* 2015, 527 (7576), 118–22.
- (44) Sudhamalla, B.; Dey, D.; Breski, M.; Islam, K. A rapid mass spectrometric method for the measurement of catalytic activity of teneleven translocation enzymes. *Anal. Biochem.* **2017**, *534*, 28–35.
- (45) Greiner, D.; Bonaldi, T.; Eskeland, R.; Roemer, E.; Imhof, A. Identification of a specific inhibitor of the histone methyltransferase SU(VAR)3–9. *Nat. Chem. Biol.* **2005**, *1* (3), 143–5.